Restoring initial conditions in a deep argillaceous formation with induced suction on retrieval

Nuria Sau[1,2]*, *Enrique* Romero[1,2], and *Hervé* Van Baelen[3]

[1]Centre Internacional de Mètodes Numèrics en Enginyeria CIMNE, Barcelona, Spain
[2]Universitat Politècnica de Catalunya UPC, Barcelona, Spain
[3]ONDRAF/NIRAS, Brussels, Belgium

Abstract. The deep and plastic Ypresian clays (Ycs) are one of the potential host rock formations in Belgium for the geological disposal of heat-emitting radioactive waste. Consequently, their thermo-hydro-mechanical behaviour has to be exhaustively studied at different depths. With this aim and considering that there is no underground research facility, deep core samples of Ycs have been retrieved between 300 and 450 m depth. The water-undrained sampling induces high matric suctions on the retrieved samples despite their nearly saturated state. Microstructural features, and particularly the larger dominant pore sizes with relatively low air-entry values, may also affect this induced suction. An experimental campaign has been launched to analyse the induced suction at different depths, which is complemented with pore size distributions carried out with mercury intrusion porosimetry. The study is accompanied by a constant volume test, in which a retrieved cylindrical sample with high initial suction is subjected to positive water pressure at the bottom boundary. The evolution of pore water pressure and total stress at different heights allows detecting the development of effective stress (swelling pressure) close to the initial suction. Finally, the paper emphasises the importance of following adequate experimental protocols on these high-suction samples to restore *in situ* conditions.

1 Introduction and background information

The Ypresian clays Ycs are a deep plastic argillaceous formation, which–together with the Boom Clay–are currently considered in Belgium for the geological disposal of heat-emitting radioactive waste. Unlike the Boom Clay, there is no underground research laboratory enabling a more accessible sampling. Therefore, to study the thermo-hydro-mechanical properties and their variability with depth, core samples of Ycs have been retrieved between 300 and 450 m below ground at Kallo (Belgium).

The water-undrained unloading upon sampling induces matric suction despite the saturated or nearly saturated state of the material after retrieval, which is associated with the null effective stress change during the process (e.g. [1,2]). This suction increase is particularly remarkable in the water-undrained and deep sampling in argillaceous formations [3]. Within this context, Table 1 summarises the sampling depth, the measured total suction, ψ, and the degree of saturation, S_r, of retrieved samples from different potential argillaceous host rock formations in Europe and reported by various authors.

It is expected that the microstructural features–particularly the largest dominant pore sizes with low-air entry values–also have some impact on these high-

induced suctions. Table 1 also incorporates information on the mono-modal or multi-modal character of the pore size distribution (PSD) by mercury intrusion porosimetry, the maximum dominant pore size, ϕ_{max}, and the air-entry value (AEV) of these dominant pores according to the Young–Laplace equation for capillary pressure. As indicated by [4], the induced suction should be compared with the capability of the porous media–mainly associated with the AEV–to sustain this value under saturated conditions. If the induced suction is larger than the AEV, then air is expected to enter the soil during retrieval (causing the decrease of S_r). If not, then the material is able to sustain the induced suction, and $S_r=1$ will be maintained.

It is important to highlight that besides the induced suction due to total stress release, some small soil water evaporation during storage may occur rendering further suction increase. This behaviour can be observed in Table 1 on the first three low-porosity formations with high AEV, in which total suctions greater than the estimated ones by the depth of retrieval and larger than the AEVs can be achieved with small water content losses.

The plastic Boom Clay is the most similar formation to Ypresian clays, albeit at a shallower depth. As can be observed in the table, the suction measured in Boom Clay (equivalent to the induced one at the sample depth) can be sustained due to its relatively high AEV (4.8

---

* Corresponding author: nuria.sau@upc.edu

MPa) and S_r can be kept close to one. The deeper Ycs display a different response associated with their larger pores: the higher induced suctions cannot be sustained due to the lower AEVs of the formation.

This paper sheds light on these as-retrieved suctions with depth by relying on a series of tests carried out on Ycs by [5]. The objective of this study focuses on

- comparing the estimated induced matric suctions and the measured ones throughout the sampling depth;

- studying the influence of the microstructural features on the measured matric suctions after retrieval; and

- highlighting the importance of following strict protocols on these high-suction samples to restore *in situ* conditions.

Table 1. Data from different argillaceous host rock formations in Europe.

Material	Ref.	Depth (m)	ψ (MPa)	S_r	PSD shape	ϕ_{max} (nm)	AEV (MPa)
Opalinus clay (Switzerland)	[6]	879	4	Close to 1	Mono-modal	16	18
	[7]	936	44	Close to 1		<8	>37
	[8]	855 – 891	67	0.73		7	42
Brown Dogger (Switzerland)	[6]	776	5	Close to 1	Mono-modal	20	14
	[9]	781	37	0.95-1.0		22	13
	[10]	767 – 778	45	0.89		16	18
COx claystone (France)	[11]	479	34	0.77	Mono-modal	32	9.1
Boom Clay (Belgium)	[9]	223	2.5	Close to 1	Mono-modal	70	4.8
Ypresian clays (Belgium)	[5]	283 – 390	1.5-3.2	0.82-1.0	Multi-modal and mono-modal	81 - 2075	0.15-3.9

2 Suction and microstructural depth profiles in Ypresian clays

The Ycs are a sequence of marine sediments deposited during the Ypresian Age (spanning the time between 56 to 47.8 Ma). An exhaustive experimental study on core samples retrieved along 100 m depth (from 283 to 390 m) at Kallo (Belgium) has been reported by [5] to assess the natural variability of the mineralogy, bulk density and microstructural features.

This section summarises selected results on six core samples using Mercury Intrusion Porosimetry (MIP) tests and measurements of the initial total suction using a chilled-mirror dew-point psychrometer (WP4). The results will help better understanding the role played by the microstructural features.

The induced matric suction after retrieval can be estimated assuming perfect sampling (no mechanical disturbances during sampling, storage and trimming), which implies that the release of mean total stress, Δp, is equal to the decrease in pore water pressure, Δu_w (i.e. null effective stress change during the process). Total and effective vertical stresses, σ_{vi} and σ_{vi}', and the pore water pressure, u_{wi}, at *in situ* conditions were determined assuming a homogeneous bulk density throughout the studied depth (1.97 Mg/m³ [12]) with a water-table elevation at ground surface. The same earth pressure coefficient at rest K_0^{SC} [13] was considered, assuming a yield stress ratio YSR=1.4 [12] and a drained friction angle ϕ'=16° [14] along the 100 m of Ypresian clays:

$$K_0^{SC} = (1 - \sin\phi')\sqrt{YSR} = 0.86 \qquad (1)$$

The mean effective and total stresses, p_i' and p_i, at *in situ* conditions were

$$p_i' = \frac{1}{3}(1 + 2K_0^{SC})\sigma_{vi}' \; ; \; p_i = p_i' + u_{wi} \qquad (2)$$

After retrieval, $p_f = 0$, and the decrease in pore water pressure is equal to $\Delta u_w = -p_i = -(p_i' + u_{wi})$. Therefore, the matric suction after retrieval was determined as

$$s = -u_{wf} = -(u_{wi} + \Delta u_w)$$

(3)

An alternative to these analyses when the degree of saturation is slightly less than one could be using Skempton's pore pressure parameters [15]. For example, the isotropic pore pressure parameter for incompressible solid can assumed B=0.91 based on an average bulk compressibility of the soil skeleton 2.0×10^{-6} m²/kN and average porosity n=0.44 along a water undrained path to restore *in situ* conditions [5].

Particular care has been taken to evaluate the matric suction, s, from the measured (with WP4) total initial suction, ψ, and to consider an estimated osmotic suction, π, that evolves with the degree of saturation, S_r. The degree of saturation has been introduced to take into account solvent evaporation and the corresponding increase in salinity. The pore water of Ycs is mainly

composed of sodium chloride NaCl and sodium sulphate Na_2SO_4. The osmotic component was determined using the following expression [16] that considers salt mass concentration, C_0, of the heteroionic Ycs solution.

$$\pi = 68.3 \text{ kPa} \left(\frac{1}{S_r} \frac{C_0}{1 g/L} \right)^{1.014} = \frac{541 \text{ kPa}}{S_r^{1.014}} \qquad (4)$$

where C_0=7.7 g/L was assumed homogeneous throughout the profile.

Figure 1a plots the depth profile of the estimated induced matric suctions on each core sample (labels on the plot), as well as the measured total suctions corrected by the osmotic component. It is worth noting that the estimated values are consistently higher than the measured ones. Moreover, core samples after retrieval consistently displayed degrees of saturation below 0.95, as plotted in Figure 1b. This fact is probably associated with the high matric suctions induced on retrieval– between 2.5 and 3.5 MPa– and the pore size distribution of Ycs. The results of MIP tests on freeze-dried samples allow plotting the depth profiles in Figure 2a of the maximum dominant pore sizes. The corresponding air-entry values AEVs based on these dominant pore sizes and estimated using the Young–Laplace equation are shown in Figure 2b.
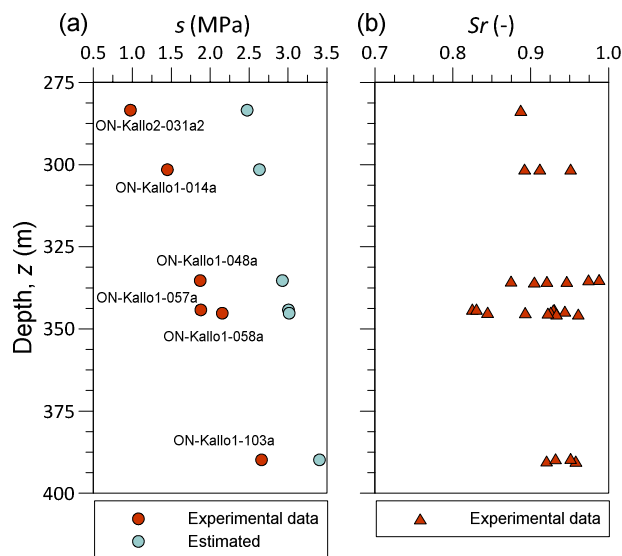

Fig. 1. Depth profiles: (a) induced (estimated) matric suctions on retrieval and measured ones; and (b) measured degrees of saturation.

All core samples display multi-modal pore size density functions except one mono-modal at 390 m depth (ON-Kallo1-103a), with dominant maximum pore sizes ranging between 100 nm and 2 µm, and AEVs between 0.15 and 3.15 MPa. The smallest AEV corresponds to a sandy sample and the largest to the clayey sample with the mono-modal distribution.

AEVs are consistently lower than the estimated matric suctions, even in the case of the sample with mono-modal distribution and dominant pore size of 100 nm. Consequently, and despite the careful sampling and trimming, some air is expected to enter the soil. This

air induces some small swelling of the material. Typically a compression deformation of around 0.77% has been observed under oedometer conditions on restoring the *in situ* vertical effective stress [5].
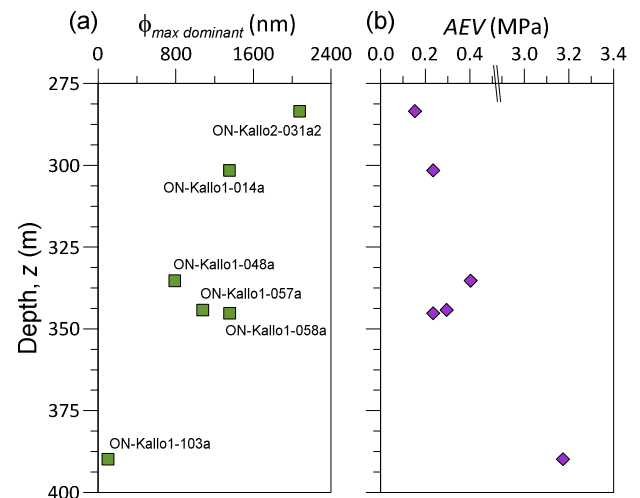
Fig. 2. Depth profiles: (a) maximum dominant pore sizes from MIP; and (b) estimated air-entry values using Young–Laplace equation.

It is important to point out that it is anticipated that the sample will not become homogeneously desaturated during preparation. Only the external surface of the 100 mm core may be the most susceptible zone to air entry and drying during trimming. Afterwards, vacuum packing will allow the suction, and therefore the degree of saturation, to be homogenised.

3 Sample tested under constant volume

The constant volume (isochoric) test was performed on a sample retrieved at 334.8 m depth (core ON-Kallo1-048a). The Ycs at this depth present 48% clay minerals, which are dominated by smectite (25.4%) and illite (13.4%). Non-clayey fraction is mainly constituted by quartz (35%), alkali feldspar (3.6%) and plagioclase (5.1%) [17]. Table 2 summarises the soil properties, the initial state of the sample and the AEV determined by MIP.

Figure 3 shows the multi-modal pore size distribution. The maximum intruded void ratio was 0.686, which indicated a quite connected pore network close to the void ratio reported in Table 2. Three dominant pore sizes were detected with a maximum value of 780 nm associated with a low air-entry value of 0.40 MPa. The induced matric suction on retrieval (close to 3 MPa as shown in Figure 1a) cannot be sustained, and air entry is expected to occur (S_r=0.875).

Figure 4 displays the water retention curve on drying in terms of matric suction. The total suction results using WP4 psychrometer have been corrected for the osmotic component according to Equation (4). Results have been fitted to the van Genuchten equation [18]. The plot also includes the initial state of the sample that approximately matches the fitted curve. The figure also provides water retention results obtained from MIP. The procedure

proposed by [19] has been followed to ensure that measured data and estimated data from MIP are consistent at $s \approx 3$ MPa (i.e. within the capillary domain).

Table 2. Properties and the initial state of the tested material.

Soil properties	Core ON-Kallo1-048a (depth: 334.8 to 335.8 m)
Bulk density, ρ	1.91 Mg/m^3
Density of solids, ρ_s	2.72 Mg/m^3
Water content, w	25.2 %
Void ratio, e	0.785
Degree of saturation, S_r	87.5 %
Total suction, ψ	2.4 MPa
Matric suction, s	1.8 MPa
Air-entry value, AEV	0.40 MPa
Particle sizes < 40 µm	99.8 %
Particle sizes < 2 µm	31.3 %
Liquid limit, w_L	134 %
Plasticity index, PI	105 %
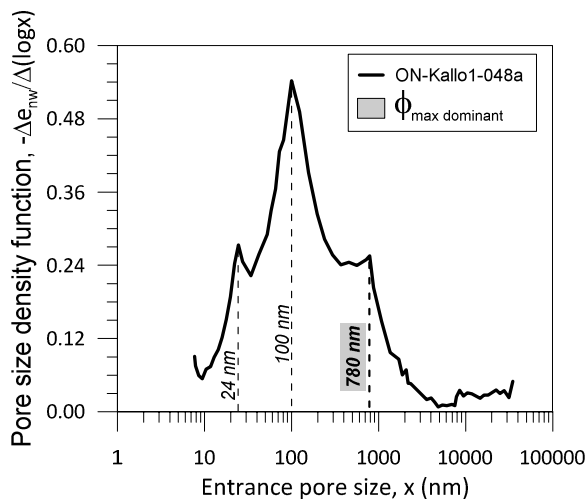
Fig. 3. PSD obtained by MIP on a freeze-dried sample from core ON-Kallo1-048a.
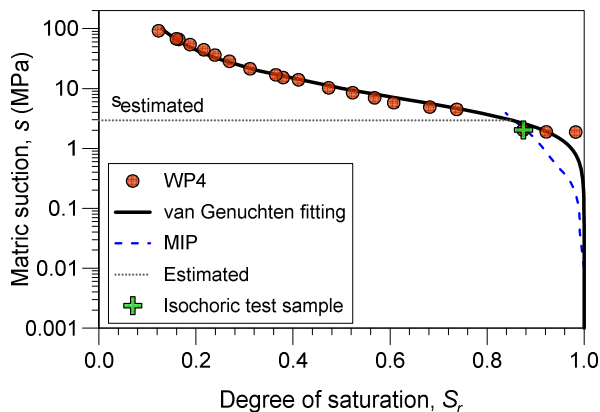

Fig. 4. Drying retention curves of core ON-Kallo1-048a in terms of matric suction. The plot includes the fitted curve, the water retention curve deduced from MIP data and the initial state of the sample.

4 Swelling pressure test by reducing the induced suction on retrieval

The soil sample previously described has been installed in a cylindrical constant volume cell (75 mm in diameter and 100 mm high). The sample displays bedding planes orthogonal to the axis of symmetry of the cell. The aim of the test focuses on measuring the final vertical and horizontal effective stresses developed on reducing the induced suction associated with deep retrieval and some drying. At constant volume and S_r close to one, the initial effective stress is expected to coincide with the final one after contact with water and the application of backpressure. The initial effective stress (at null total stress and $S_r \approx 1$) corresponds to $\sigma'_i = -u_{wi} = s_i$ (i.e. $\sigma'_i = 1.8$ MPa according to Table 2).

The isochoric cell was developed by [20], updated by [12] and recently improved with total stress sensors by [5,21]. Figure 5 shows two schematic cross-sections of the isochoric cell. It allows continuous monitoring at specific points of the boundaries of pore water pressures (Pw_1 and Pw_2 at 75 and 25mm from the bottom, respectively), temperatures (T_1 and T_2) and total stresses (P_1 and P_3 at mid-high on opposite sides, and P_2 at the top of the sample). The hydraulic boundary conditions (top and bottom valves, u_u and u_b) are independently controlled using two volume/pressure controllers.
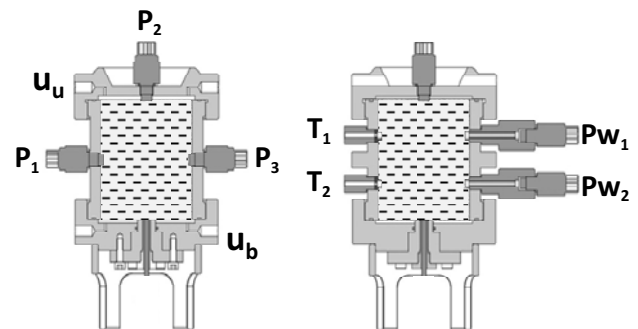

Fig. 5. Schematics of the improved isochoric cell with pore pressure transducers (Pw_i), total stress sensors (P_i), thermocouples (T_i), and water inlet (u_b) and outlet (u_u).

The hydration of the soil sample has been performed by applying a step-wise water pressure increase 0.1, 0.3, 0.5 and 1 MPa at the bottom valve (u_b), while the upper valve (u_u) has been kept under atmospheric conditions. At the end of the hydration, the upper valve (u_u) was closed, ensuring uniform water backpressure of 1 MPa in the sample. Figure 6 and Figure 7 show the time evolution of pore water pressures and total stresses, respectively, during the different steps. As observed in Figure 6, it took some time for the transducers to record positive water pressures after applying the water backpressure at the bottom of the sample (Pw_2 after 6 days and Pw_1 after 19 days). This delay in the response is associated with different aspects. On the one hand, the initial suction needs some time to develop into the positive range (saturation of the material). On the other hand, additional time is required to fill the lines and porous discs that interact with the transducer, particularly when the sensors are placed in a horizontal

orientation with the possibility of trapping air. Given this experience, pre-filling the connector and transducer with water during the assembly of the cell will overcome such delays. The steady-states recorded by the water pressure transducers with u_u valve at atmospheric pressure appear to follow a linear pore pressure distribution with height (consistent with a uniform water permeability). Once u_u is closed, Pw_1 and Pw_2 show a relatively rapid increase to the target backpressure associated with a correct saturation of the sample.

The time-evolution of total stresses is consistent with the backpressure applied at the bottom of the sample during the different steps. The development of total stresses is related to the reduction of suction at constant volume conditions, as well as to the backpressure applied (constant effective stress). Once u_u is closed, and the equalisation of pore water pressures is reached, the values of swelling pressure (total stresses minus pore pressures) can be obtained. Some anisotropy is observed during the saturation and suction reduction process, since a maximum vertical effective stress of 1.23 MPa (P_2) in the direction orthogonal to the bedding planes is detected. The horizontal effective stresses reached values of 0.45 and 0.33 MPa (P_1 and P_3).
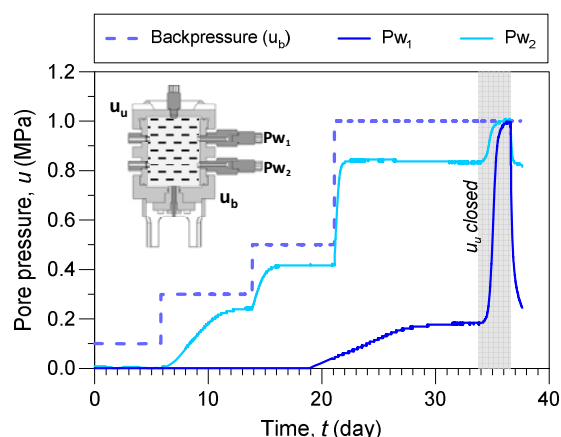
Fig. 6. Time evolution of pore water pressures at different locations during the hydration and backpressure steps.
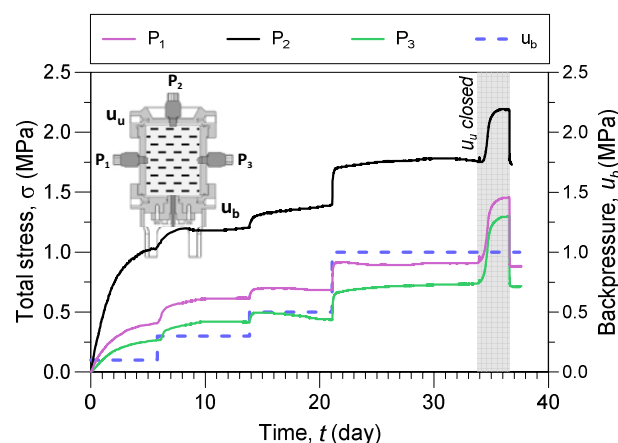
Fig. 7. Time evolution of total stresses at different locations during the hydration and backpressure steps.

Table 3 summarises the applied hydraulic boundary conditions and the maximum pore water pressures and total stresses measured during each step. The maximum vertical effective stress of 1.23 MPa (swelling pressure at the final step) is close to the induced (initial) matric suction of 1.8 MPa (Table 2).

Table 3. Pore water pressures Pw_i and total stresses P_i at the end of the backpressure (u_b) steps. All units in MPa.

u_b	u_u	Pw_1	Pw_2	P_1	P_2	P_3
0.1		0.00	0.00	0.40	1.03	0.26
0.3	Open	0.00	0.24	0.61	1.20	0.41
0.5		0.04	0.42	0.68	1.39	0.44
1		0.19	0.84	0.91	1.76	0.74
1	Closed	1.00	1.00	1.45	2.23	1.33

At the end of the test, the backpressure has been quickly reduced in one step, followed by the opening of u_u and u_b valves to atmospheric pressure. Then the soil sample has been carefully removed from the cell, displaying a slight swelling. Three specimens were immediately trimmed at different heights for total suction measurement. The final induced matric suction on water undrained unloading is approximately constant throughout the sample height, displaying values 0.78, 0.84 and 0.64 MPa. The average induced matric suction is also close to the average value of swelling pressure (effective stress) measured in the test (around 0.7 MPa).

5 Concluding remarks and comments on restoring *in situ* conditions

The plastic and deep Ypresian clays Ycs are currently considered in Belgium–together with the Boom Clay–potential argillaceous formations for the geological disposal of heat-emitting radioactive waste. Selected experimental results from an exhaustive test programme reported by [5] on Ycs core samples retrieved along 100 m depth (from 283 to 390 m) at Kallo (Belgium) are used in the current study. The data have allowed comparing the estimated induced matric suctions on water undrained sample retrieval–assuming perfect sampling–and the measured ones in the laboratory after careful sample extraction and trimming.

The depth profiles of the estimated induced matric suction on retrieval, as well as the measured total suction corrected by the osmotic component, show that the estimated values–between 2.5 and 3.5 MPa–are consistently higher than the measured ones–between 1.0 and 2.7 MPa. This fact has led to the assumption that such a high induced matric suction has not been able to be sustained by the size of the largest dominant pores. This is the rationale behind the completion of the study with mercury intrusion porosimetry tests on freeze-dried samples to analyse the influence of these largest pores with the lowest air entry values AEVs.

Most studied core samples display multi-modal pore size density functions with maximum pore sizes ranging

between 100 nm and 2 µm, and AEVs between 0.15 and 3.15 MPa. The AEVs are consistently lower than the estimated matric suctions. It is anticipated that these large pores desaturate (inducing some air entry) and consequently some small expansion of the sample. Moreover, core samples after retrieval consistently display degrees of saturation below 0.95.

A constant volume test has been performed on a sample retrieved at mid-depth of the formation with an initial matric suction of 1.8 MPa and degree of saturation 0.875. The aim of this test focuses on measuring the final vertical and horizontal effective stresses developed on reducing the induced suction associated with deep retrieval and some drying. Some anisotropy is observed during the saturation and suction reduction process, since a maximum vertical effective stress of 1.23 MPa–close to the initial matric suction–in the direction orthogonal to the bedding planes is detected. In contrast, the horizontal effective stresses reached values of 0.33 and 0.45 MPa. The final matric suction after fast (water undrained) unloading is approximately constant throughout the sample height (between 0.64 and 0.84 MPa), which is similar to the mean swelling pressure measured in the test (0.69 MPa).

The induced suction on water undrained retrieval should be considered for the definition of the stress paths to follow since samples can undergo swelling and possible degradation on contact with water at low stresses [4]. Samples should be loaded to total stress slightly higher than the *in situ* effective stress, and only then, placed in contact with synthetically prepared water at atmospheric pressure and equivalent osmotic suction.

Acknowledgements

References

1. A. W. Skempton, V. A. Sowa, Géotechnique **13**, 269 (1963).

2. I. G. Doran, V. Sivakumar, J. Graham, A. Johnson, Géotechnique **50**, 189 (2000).

3. P. Delage, T. Le, A.-M. Tang, Y.-J. Cui, X.-L. Li, Géotechnique **57**, 239 (2008).

4. A. Ferrari, E. Romero, Geophys. Monogr. Ser. Am. Geophys. Union (2019).

5. N. Sau, Thermo-Hydro-Mechanical Behaviour of Deep Argillaceous Formations (in Progress), 2020.

6. E. Romero, R. Gómez, *Water and Air Permeability Tests on Deep Core Samples from Schlattingen SLA-1 Borehole. NAB 13-51* (Wettingen, Switzerland, 2013).

7. E. Romero, L. Gónzalez-Blanco, *Complementary Water and Air Permeability Tests on Core Samples from Schlattingen SLA-1 Borehole. NAB 15-06* (2015).

8. A. Ferrari, L. Laloui, in *Multiphysical Test. Soils Shales. Springer Ser. Geomech. Geoengin.*, edited by L. Laloui and A. Ferrari (Springer, Berlin, Heidelberg, 2013), pp. 57–58.

9. L. Gonzalez-Blanco, E. Romero, C. Jommi, X. Li, X. Sillen, Geomech. Energy Environ. **6**, 81 (2016).

10. A. Ferrari, V. Favero, P. Marschall, L. Laloui, Int. J. Rock Mech. Min. Sci. **72**, 61 (2014).

11. P. Delage, H. Menaceur, A.-M. Tang, J. Talandier, in *3rd Eur. Conf. Unsaturated Soils. E-UNSAT 2016* (E3S Web of Conferences, Paris, France, 2016), p. 18004.

12. A. Lima, Thermo-Hydro-Mechanical Behaviour of Two Belgian Clay Formations: Boom and Ypresian Clays, Universitat Politècnica de Catalunya, 2011.

13. G. Della Vecchia, A. Lima, C. Jommi, E. Romero, in *Proc. 5th Int. Conf. Unsaturated Soils* (Barcelona, Spain, 2010), pp. 803–809.

14. X. P. Nguyen, Y. J. Cui, A. M. Tang, X. L. Li, *Ypresian, THM Behaviour of Clay. 4th Ypresian Clay Meeting* (Barcelona, Spain, 2011).

15. A. W. Skempton, Géotechnique **4**, 143 (1954).

16. C. Mata, E. Romero, A. Ledesma, in *3rd Int. Conf. Unsaturated Soils, UNSAT*, edited by J. F. T. Jucá, T. M. P. de Campos, and F. A. M. Marinho (Recife, Brazil, 2002), pp. 283–288.

17. G. Mertens, R. Adriaens, *Analysis Report of the Bulk and Clay Mineralogy of 21 ON-Kallo-1 Samples* (2018).

18. M. T. van Genuchten, Soil Sci. Soc. Am. J. **44**, 892 (1980).

19. E. Romero, P. H. Simms, Geotech. Geol. Eng. **26**, 705 (2008).

20. J. Muñoz, E. E. Alonso, A. Lloret, Géotechnique **59**, 293 (2009).

21. N. Sau, E. Romero, H. Van Baelen, in *7th Int. Symp. Deform. Charact. Geomaterials* (EDP Sciences, Glasgow, United Kingdom, 2019), pp. 1–6.